SHORELINE BASED FEATURE EXTRACTION AND OPTIMAL FEATURE SELECTION FOR SEGMENTING AIRBORNE LIDAR INTENSITY IMAGES

Michael J. Starek[2], Raghav K. Vemula[2], K.Clint Slatton[1, 2], Ramesh L. Shrestha[2], and William E. Carter[2]

1: Department of Electrical and Computer Engineering
2: Department of Civil and Coastal Engineering
University of Florida
E-mail: slatton@ece.ufl.edu, mstarek@ufl.edu

ABSTRACT

Modern airborne laser swath mapping (ALSM) systems measure both elevation and reflection intensity of the terrain. However, this intensity has been under utilized as a feature for image classification because it does not represent true terrain radiance. In areas with minimal topographic relief, such as beaches, we show that segmenting intensity images rather than elevation images has great potential for scene analysis. Several intensity-based features are extracted from ALSM data collected along a beach and partitioned into three classes to detect the water line. Class-conditional probability density functions are estimated for each feature to asses which are most informative. Results indicate significant class separation using centroidal features. Their classification performance is evaluated using a naïve Bayes classifier and the area under receiver operating characteristic curves. The method presented provides a novel feature extraction and a systematic feature selection procedure for high-resolution ALSM intensity data.

Index Terms — laser radar, feature extraction, image segmentation, image classification, entropy

1. INTRODUCTION

Airborne laser swath mapping (ALSM), often referred to as light detection and ranging (LiDAR), enables sub-meter spatial sampling of topography. An ALSM system pulses a near-infrared laser from an airborne platform to the ground several thousand times per second. By precisely determining the position and attitude of the aircraft as well as the angle at which each laser pulse leaves the aircraft, the direction of the laser pulse toward the ground can be accurately calculated. Combining this information with the recorded return time of the reflected pulse allows for a three-dimensional point sampling of the ground and landcover [1]. From the resulting ALSM point data, digital images are created in which the pixel value corresponds to the mean topographic elevation of the points within that pixel. These images often exhibit rms elevation errors of less than 10cm over minimally-vegetated surfaces, such as beaches. For most ALSM systems, the points also have associated intensity values, which can be similarly interpolated into an intensity image. To date, the intensity values have rarely been utilized by earth scientists, largely because they are only recorded as relative values. Thus, they are unitless and do not represent absolute surface radiance.

For most ALSM systems, intensity is defined as the ratio of return pulse energy to that of transmitted pulse energy, and is related to the pseudoreflectance of the ground or object the laser spot illuminates. ALSM intensity measures are affected by the following factors: variations in path length, surface roughness and orientation (local incidence angle), beam divergence, object composition, object density, saturation from background reflections, and attenuation of the signal through the atmosphere. Generally, ALSM intensity values are normalized for path length variations before generating an image [2]. Although the reflectance cannot be converted to a true radiance for the object, we demonstrate that relative intensity measures can still provide useful information for image segmentation and classification.

Some researchers have assessed the possibility of using the intensity information from airborne laser data for classification and image generation. [3] evaluated the suitability of airborne laser intensity data for land cover classification. [4] investigated airborne laser intensity on glacial surfaces utilizing comprehensive laser geometry modeling and orthophoto surface modeling. [2] found highly effective classifications of buildings and trees from ALSM features derived from intensity.

In this analysis, the potential of ALSM intensity as a feature for improved beach-zone image segmentation is assessed. A brief description of the data and the numerical approach used to generate digital images and extract features is presented in Section 2. Section 3 introduces the analysis methods used to rank PDF feature separation based on entropy divergence measures. Section 4 presents the

results of the analysis and Bayes classification performance. Conclusions are presented in Section 5.

2. APPROACH

The data set investigated was collected by the University of Florida (UF) on January 27, 2006 for the St. Augustine Beach, FL and surrounding region. The survey was conducted at approximately low tide using UF's Optech ALTM 1233 airborne laser scanning system. This area was selected since geo-referenced aerial imagery was collected on the same flight as the ALSM data. The high-resolution imagery enables ground truth labeling for segmenting the intensity image into various beach classes for training.

2.1 Automated profiling and data segmentation

Once the data set was obtained, the raw ALSM intensities were normalized using a UF-developed program [5] to correct for intensity variations due to changes in path length and then interpolated into a 1m digital intensity image with 1m pixel resolution. Ordinary geo-statistical Kriging was used for the interpolation with a linear variogram and nugget effect to account for systematic error of ~7cm in the vertical, determined by the precision of the GPS trajectory for the airplane [6]. The aerial imagery, which was georeferenced to the same coordinate frame as the ALSM imagery, was used to segment the intensity image into three classes: dry beach, wet beach, and water. All three classes are visible in the imagery (see Figure 1). Since coincident imagery is not generally available with ALSM data sets, it is important to assess the separability of these classes in the ALSM intensity data.

A compute routine was developed to mine the image by extracting intensity values along cross-shore profile lines oriented roughly orthogonal to the shoreline. This provides the *x*,*y*-coordinate and intensity value along each profile in 1m increments. These profile lines are extracted every 2m in the along-shoreline (parallel) direction and extend in the cross-shore (perpendicular) from the dune line to 10m past the water line. Once the profiles are extracted, each profile line was then segmented into each of the three classes: dry beach, wet beach, and water using the ground-truth imagery.

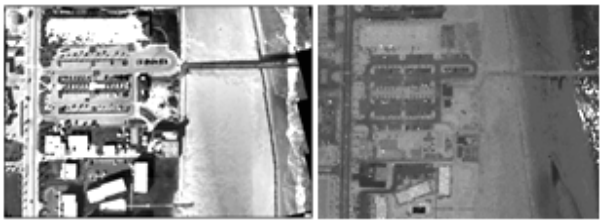

Figure 1: (Left) 500m×400m aerial photograph of study site. (Right) Intensity image derived from ALSM data. Intensity is an 8 bit unitless ratio. Dark pixels have low reflectance. Some data dropout can be seen on the breaking waves.

2.2 Feature extraction

Once the profiles were extracted and classified into dry, wet, and water, several features based on intensity were then computed for each profile line on a per class basis. Take for example a hypothetical feature, f_1. Then for profile l_1, values for f_1 are computed separately for the profile points in each class C_i for $i = \{1,2,3\}$. Since all three classes are present in all profiles, we obtain $f_1(l_m, C_1)$ for feature 1 and class 1, where m indexes the profile number. Results are accumulated over all features, profiles, and classes. This approach allows us to examine interclass separation and class-conditional probabilities $p(f_j|C_i)$ for $i = \{1,2,3\}$ and j indexing the feature set.

The following features are mined from the intensity profiles: minimum intensity, maximum intensity, median intensity, mean intensity, standard deviation of intensity, mean curvature, mean gradient, intensity slope.

Most of the aforementioned features are self-explanatory, but some require further detail. Mean gradient is based on computing a local gradient every 2 meters along the intensity profile, which is smoothed using a moving average filter of window size 5, and then taking the mean of those gradient values. The gradient was computed using a centralized-difference approximation. The mean curvature was computed as the gradient of the gradient values and then taking the mean value for that profile. The intensity slope was computed using a regression line through the profile points.

There are other feature measures that can be derived from intensity data, such as texture measures. However, many of these measures are based on image processing techniques that require moving windows. As explained previously, our features are extracted from the values along a profile line as opposed to using a moving 2D window or data clustering. This approach was selected to stay consistent with the standard practices used in coastal erosion studies, which utilize cross-shore and along-shore measurements as the most natural coordinate frame. Traditional methods are generally based on manually surveyed cross-shore profiles spaced at equal intervals. The major difference is that ALSM offers several orders of magnitude higher sampling density as compared to manual surveying methods.

3. ANALYSIS

Once the features are computed for each class, their class-conditional probability density functions (PDFs) are used to assess the PDF separability using divergence measures. The features that correspond to the most separable PDFs are

more likely to yield robust classification. Figure 2 shows class-conditional PDFs (likelihoods) for the median intensity feature. As observed in these plots, the data in feature space are multi-modal and non-Gaussian in appearance, as is often the case with ALSM data. Therefore, the non-parametric Parzen windowing method was selected to estimate the PDFs from the data. The Parzen windowing method uses a *d*-dimensional histogram to estimate the probability density $p_n(\vec{x})$ [7] as

$$p_n(\vec{x}) = \frac{1}{n}\sum_{i=1}^{n}\frac{1}{h_n^d}\varphi\left(\frac{\vec{x}-\vec{x}_i}{h_n}\right) \quad (1)$$

where n is number of points for feature x, and h_n is the edge length of a hypercube in feature space. d=1 for this analysis since we extract 1D profiles. φ is the window function and was chosen to be a univariate Gaussian window since the features can be spatially correlated [7]:

$$\varphi(u) = \frac{1}{\sqrt{2\pi}}e^{-u^2/2} \quad (2)$$

Crucial to Parzen estimation is the selection of the edge length, h_n. If h_n is too large it over smoothes the data, and if it is too small φ approaches a delta function and the PDF estimate tracks the samples too closely. A reasonable value for h_n was determined empirically to be 1/30th of the range of values for each feature.

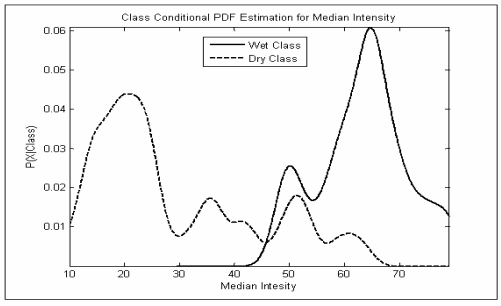

Figure 2 Class-conditional PDFs estimated using Parzen windowing for median intensity. Notice the non-Gaussian, multi-modal nature of data that necessitates a non-parametric PDF estimation approach.

Generally, the more separation between classes for a given feature, the more probable that feature will lead to successful classification. To assess inter-class separation across the estimated likelihoods, two performance metrics based on relative entropy, i.e. the Kullback-Leibler divergence (Dkl), are used: Jensen-Shannon divergence (JSD) and a normalized form of JSD. The JSD has the following form [8]:

$$JSD(P,Q) = \frac{1}{2}\left[D_{kl}\left(P,\frac{P+Q}{2}\right) + D_{kl}\left(Q,\frac{P+Q}{2}\right)\right] \quad (3)$$

where P and Q are the conditional PDFs of a feature under two different classes. JSD is a symmetric form of Dkl and is non-negative. By taking the square root of the JSD it satisfies the triangle inequality and all other properties of a metric [8]. The square root form of JSD is often used for feature selection in classification problems. Therefore, $\sqrt{\text{JSD}}$, referred to hereafter simply as JSD, was selected as a measure to assess feature discriminability.

When assessing which features provide more divergence between classes using entropy-based measures, such as Dkl, one must be cautious. Some features may have larger inherent entropies and this can pose problems when comparing across different feature spaces. The standard Dkl definition of the divergence is biased towards large entropies [9]. Hence, we also use a form of JSD that is normalized by the entropy of P and Q:

$$NJSD(P,Q) = \left[\frac{D_{kl}\left(P,\frac{P+Q}{2}\right)}{2H(P)} + \frac{D_{kl}\left(Q,\frac{P+Q}{2}\right)}{2H(Q)}\right]^{1/2} \quad (4)$$

where H is entropy. This metric is referred to as the *normalized-JSD* (NJSD).

The spatial arrangement of classes in the cross-shore seaward direction is dry beach, wet beach, and then water. Thus, we can treat the 3-class problem as two 2-class problems. The classification performance of each feature was tested using a two-class *naïve Bayes* classifier and *k*-folds cross-validation [7], which is a method that randomly divides the data into a test and training set *k* times. This provides a means to test generalization capabilities for each feature with the limited training data.

Receiver operating characteristic (ROC) curves were generated for each feature for each of the *k* classifications. ROC curves depict classifier performance as a function of decision threshold x^* in which the true positive rate $p\left(x > x^* \middle| x \in C_2\right)$ is plotted on the Y axis and false positive rate $p\left(x > x^* \middle| x \in C_1\right)$ is plotted on the X axis. By varying a threshold, ROC curves for the classifier can be generated. Figure 3 below displays example ROC curves for three features used for wet beach vs. dry classification. The diagonal line represents random guessing. An important property of ROC curves is that they're insensitive to changes in prior class distributions [10].

To evaluate classifier performance between features the area under the curve (AUC) was calculated for each of the resulting *k* ROC curves for each feature using trapezoidal integration and then averaged. AUC is a scalar measure and varies between 0 for no classification success, 0.5 for random guessing, to 1 for perfect classification results. The AUC is equivalent to the Wilcoxon test of ranks [10]. Thus, we expect those features determined to be most separable to provide the best classification performance and have an

AUC close to 1. In this regard, the AUC acts as a measure of feature separation.

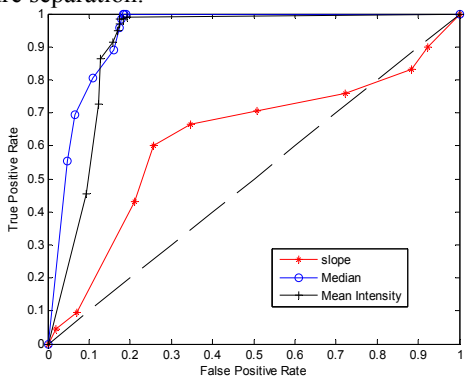

Figure 3 *k*-averaged ROC curves for wet beach vs. water. (dashed line represents performance of random guessing).

4. RESULTS

Table 1 presents separation rankings between wet and dry beach for each feature and the mean AUC results. 1 is most separable, 8 least separable. The high ranking of mean and median is expected since dry sand tends to reflect more than wet sand at the system's near-infrared wavelength of 1064 nm. Mean gradient and curvature provide the least separation as these values are texture measures. One interesting aspect is the subtle difference between JSD and NJSD rankings, such as for max and mean. These differences can be viewed as the max feature having more inherent entropy compared to the mean feature. By normalizing, the bias is accounted for, thereby resulting in the mean receiving the highest rank in NJSD.

Table 1. Dry vs. wet beach rankings

Feature	*JSD*	Rank	*NJSD*	Rank	*Avg. Rank*	*Mean AUC*
Mean	0.82052	**2**	0.34746	**1**	1.5	**1.00**
Median	0.81464	**3**	0.34334	**3**	3	**1.00**
Max	0.82086	**1**	0.34522	**2**	1.5	**1.00**
Min	0.66549	**4**	0.26951	**4**	4	**0.94**
Intensity slope	0.51744	**6**	0.20107	**5**	5.5	**0.94**
Std. dev. of intensity	0.54790	**5**	0.19063	**6**	5.5	**0.84**
Mean gradient	0.40058	**7**	0.13496	**7**	7	**0.80**
Mean curvature	0.44397	**8**	0.15160	**8**	8	**0.79**

Table 2. Wet beach vs. water rankings

Feature	*JSD*	Rank	*NJSD*	Rank	*Avg. Rank*	*Mean AUC*
Mean	0.67326	**2**	0.28762	**1**	1.5	0.90
Median	0.68117	**1**	0.28681	**2**	1.5	0.94
Max	0.56652	**3**	0.24286	**3**	3	0.86
Min	0.55742	**4**	0.23062	**4**	4	0.85
Intensity slope	0.28418	**5**	0.11357	**7**	6	0.65
Std. dev. of intensity	0.24341	**8**	0.11620	**6**	7	0.54
Mean gradient	0.26650	7	0.09774	**8**	7.5	0.54
Mean curvature	0.28322	**6**	0.11972	**5**	5.5	0.59

As expected the most separable centroidal features provide the best classification compared to texture measures as observed in the mean AUC. Maximum AUC is achieved in Table 1 for some features due to very distinct changes in surface reflectance when moving from dry to wet beach. The rankings for wet beach vs. water are presented in Table 2, where Mean and Median are again highly ranked with Median having the highest mean AUC. The measures indicate that wet beach is slightly more separable from dry beach than from water.

5. CONCLUSIONS

The potential of ALSM intensity measures for improved beach-zone image segmentation was assessed. Several features were extracted and segmented into important classes for coastal-area monitoring. Class-conditional PDFs were estimated via Parzen windowing for each feature and their inter-class separation ranked using JSD and NJSD. Based on Bayes classifications using averaged AUC, results strongly indicate that ALSM intensity measures do provide useful information for image classification. The method presented provides a systematic approach to extract features from high-resolution ALSM data over beaches that exploits the natural geometry of shorelines and a robust framework for ranking inter-class separation for feature selection.

6. ACKNOWLEDGMENTS

This work was supported in part by the NSF National Center for Airborne Laser Mapping (NCALM).

7. REFERENCES

[1] A. Wehr and U. Lohr, "Airborne laser scanning—An introduction and overview," *Journal of Photogrammetry & Remote Sensing*, vol. 54, pp. 68–82, 1999.

[2] B. J. Luzum, K. C. Slatton and R. L. Shrestha, "Identification and analysis of airborne laser swath mapping data in a novel feature space", *IEEE Geoscience and Remote Sensing Letters*, Vol. 1, No. 4, October 2004.

[3] J.H. Song, Soo-Hee Han, Kiyun Yu and Yong-Il Kim. "Assessing the possibility of land-cover classification using lidar intensity data" *ISPRS Commission III*, PCV02. 2002.

[4] E. Lutz, Th. Geist and J. Stötter. "Investigations of airborne laser scanning signal intensity on glacial surfaces - utilizing comprehensive laser geometry modeling and orthophoto surface modeling", *Proceedings of the ISPRS working group III/3*. October, 2003.

[5] B.J. Luzum, K.C. Slatton, M.J. Starek, "GEM_ Rep_ 2004_07_001", http://www.aspl.ece.ufl.edu/reports, 2004.

[6] Goovaerts, P., *Geostatistics for Natural Resources Evaluation*, Oxford Press, 1997.

[7] R. O. Duda, P. E. Hart, and D. G. Stork, *Pattern Classification*, 2nd ed. New York: Wiley, 2001.

[8] S.C. Tsai, W .G Tzeng, and H.L.Wu "On the Jensen–Shannon divergence and variational distance", *IEEE Transactions on Information Theory*, Vol. 51, No. 9, September 2005.

[9] R. K. Guha and S. Sarkar, "Characterizing temporal SNR variation in 802.11 networks", *Wireless Communications and Networking Conference*, 2006. WCNC 2006. IEEE, April 2006.

[10] T. Fawcett, "An introduction to ROC analysis", *Pattern Recognition Letters*, 27, 2006.